

Short Communication

Band Structure Research of a 2D Honeycomb Lattice Phononic Crystal

Zongyu Gao^{1,2,*}, Jianjun Fang¹, Yinong Zhang¹ lang jiang¹

¹ Beijing Union University, College of automation, Beijing 100101, China
gzy19750510@163.com

² Beijing Jiaotong University, School of Electrical Engineering, Beijing 100044, China

*E-mail: gzy19750510@163.com

Received: 28 March 2013 / Accepted: 29 April 2013 / Published: 1 June 2013

Using ultrasonic immersion transmission technique, the band gap properties of a two-dimensional honeycomb lattice/water phononic crystal were investigated both theoretically and experimentally. The band structure was calculated with the plane wave expansion (PWE) method. The results revealed that the crystals exist low frequency band gap and the frequency range of the first complete band gap is accordance with the theoretical calculation. The band degeneracy at high symmetry point in the first Brillouin zone was lifted due to increase Filling Fraction, and hence a new low-frequency absolute band gap between the first and the second bands appeared. With the normalization radii (r_0/a) increase that the first band gap relative broadband of the honeycomb array of steel cylinders in water is monotonic increase and open band gap in $r_0/a = 0.21$. The measured transmission spectra were found to be in good agreement with the numerical results.

Keywords: Phononic crystal ;Band gap ;Plane wave expansion method

1. INTRODUCTION

During the past two decades, with the development of photonic crystals and phononic crystals (PCs), there has been increasing research interest in the wave propagation characteristics through inhomogeneous materials. PCs are periodic elastic/acoustic composites which exhibit a range in frequency where elastic/acoustic wave propagation is strictly prohibited (phononic band gaps, PBGs) [1-6]. Owing to such unique and promising physical phenomenon, PCs have many potential applications such as in sound filters, acoustic-optical devices, and phonon focusing [3,6-10].

Due to the superior features of PCs resulting from the PBG, it is essential to design the crystal structures that have a large possible band gap. Many published results showed that the triangular lattice could open a wide band gap. However, the attribute of the honeycomb lattice is similar to the triangular lattice ; as for the honeycomb lattice solid/fluid (air) PC, the band gap appeared both at large filling fraction and high-frequency regime, i.e. between the second and the forth bands (Note that the third band was almost a flat line) [4]. Meanwhile, at low-frequency regime, the first and the second bands tended to degenerate at high symmetry points in the first Brillouin zone (BZ). Therefore, the band gap disappeared. Band degeneracy played an important role in restricting the opening of the band gap [11-14]. So far, several effective approaches are achieved to lift the degeneracy of bands such as by introducing the anisotropy in materials [14] or reducing the symmetry of the structure or scatters [11,12,15_17]. For example, Wang et al. [11] and Susa [12] showed that symmetry reduction was an effective way to increase or open a new photonic band gap. Martinez et al. [16] constructed a hybrid honeycomb- graphite lattice and found a number of photonic band gaps existed by varying the radii of scatters of two sub-lattices within reasonable fabrication tolerances. Weed et al. [17] found that the rounded honeycomb holes could open an optimized photonic band gap which advanced the manufacturing feasibility.

Motivated by these works, we investigated a honeycomb lattice solid/fluid PC by increasing fill fraction. Applying the plane wave expansion (PWE) method, we investigated the band structures of two-dimensional PCs consisting of stainless steel cylinders in water and compared with the sound attenuation spectra obtained by the finite element method (FEM). Then we demonstrated our results based on the well-known ultrasonic immersion transmission technique [9]. Considering existing deaf bands at higher frequency regions, we mostly investigated the lowest stop band resulting from band degeneracy. Deaf band was a mode which was antisymmetric with respect to the propagation direction of wave; hence, it could not be excited by the plane wave transducer in experiment but existed in acoustic band structures calculated by PWE, FEM, and variational method [18-21].

The material covered in this paper is the electrodeposition of nanostructured metals from aqueous electrolytes. The main focus will be on isotropic nanosized systems and monolayers. Particulate composites will be mentioned only as far as the dispersoid is added in order to stabilise the nanostructure of the matrix. Only some hints will be given at nanometric multilayered systems. The topic of electrochemical atomic layer epitaxy will be considered. Computer modeling issues have been omitted. Recent, comprehensive papers on nanomaterials, their properties and relevant analysis methods are available[22-24].

2. MODEL AND CALCULATION METHOD

The cross section of our considered PC is shown in Fig. 1(b), where the honeycomb Bravais lattice is formed by two types of honeycomb lattices. The purple dots represent a honeycomb lattice with the lattice constant $a = 2.5$ mm, while the light gray dots illustrate the same lattice constant and radius of rod as that of the former, except for a shift distance a in the y direction. Set infinite steel cylinders along the z direction. Contrasting with triangular lattice, the symmetry of the honeycomb

structure is reduced [22] . For simplicity, we set the coordinate axes as shown in Fig. 1(a).Accordingly, the basis vectors of the lattice are

$$\mathbf{a}_1 = a\sqrt{3}\left(\frac{1}{2}, \frac{\sqrt{3}}{2}\right) \quad \mathbf{a}_2 = a\sqrt{3}\left(-\frac{1}{2}, \frac{\sqrt{3}}{2}\right) \quad (1)$$

The reciprocal lattice basic vectors of the hybrid lattice are

$$\mathbf{b}_1 = \frac{2\pi}{a\sqrt{3}}\left(1, \frac{1}{\sqrt{3}}\right) \quad \mathbf{b}_2 = \frac{2\pi}{a\sqrt{3}}\left(-1, \frac{1}{\sqrt{3}}\right) \quad (2)$$

The reciprocal lattice are

$$\mathbf{G} = (2\pi/a\sqrt{3})(n_1\mathbf{b}_1 + n_2\mathbf{b}_2) \quad (3)$$

The n_1 and n_2 are integral number; the central position of scatterer are

$$\begin{aligned} \mathbf{u}_1 &= a(0, 1/2) \\ \mathbf{u}_2 &= a(0, -1/2) \end{aligned} \quad (4)$$

According to the definition of structure factor and the translation principle of Fourier, the structure factor of honeycomb lattice $F(\mathbf{G})$ are

$$\begin{aligned} F(\mathbf{G}) &= (e^{-i\mathbf{G}\cdot\mathbf{u}_1} + e^{-i\mathbf{G}\cdot\mathbf{u}_2}) \frac{1}{S_{cell}} \int_S \exp(-i\mathbf{G}\cdot\mathbf{r}) d^2r \\ &= 2\cos(\mathbf{G}\cdot\mathbf{u}_1) f \frac{J_1(|\mathbf{G}|r_0)}{|\mathbf{G}|r_0} \end{aligned} \quad (5)$$

In this work, PCs are composed of stainless steel cylinders immersed in water. The band structure of this system is investigated with the PWE method. For the solid/fluid PCs, in the absence of an external force, the equation of motion is

$$\rho \frac{\partial^2 \mathbf{u}}{\partial t^2} = \nabla \cdot (\rho c_i^2 \nabla \mathbf{u}) \quad (6)$$

Where ρ , $C_{11} = \rho c_i^2$ and $\mathbf{u} = \mathbf{u}(\mathbf{r}, t)$ are are mass density, longitudinal elastic constant, and displacement dependence on the position, respectively.

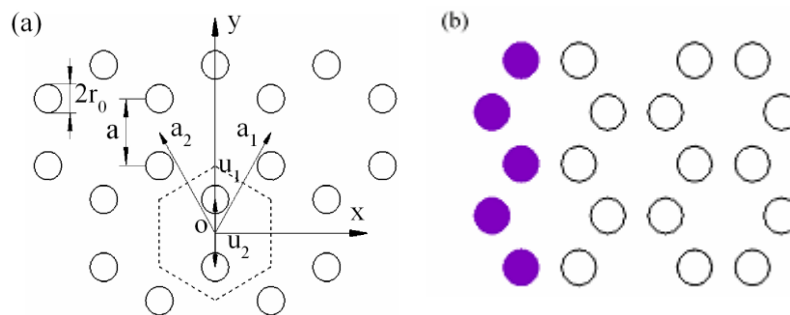


Figure 1. (a) Basis vector and unit cells of 2D steel-water phononic crystal with honeycomb lattice; (b) Schematics of cross section for a 2D honeycomb phononic crystal consisting of steel rods in water. The shadow regions show the definition of a layer

Taking advantage of the 2D periodicity and the Bloch theorem, Eq. (3) can be written as a standard eigenvalue equation. The band structure can be obtained by letting the Bloch vector scan the irreducible region of the first BZ. The detailed discussion on the PWE method is referred to in Refs. [1,4]. During the process of computation, 441 plane waves were adopted to arrive at a good convergence. The material parameters were selected as, $\rho_{\text{steel}} = 7.85 \times 10^3 \text{ kg/m}^3$

$c_l = 5940 \text{ m/s}$ for steel, and $\rho_{\text{water}} = 1.0 \times 10^3 \text{ kg/m}^3$, $c = 1480 \text{ m/s}$ for water, respectively.

3. EXPERIMENT DESCRIPTION

After that, a honeycomb lattice PC sample was designed and measured by means of the transmission experiment along the two highest symmetrical directions of the first irreducible BZ. In the experiment, the radius of steel rods (190 mm long) was taken as $r_0 = 0.75 \text{ mm}$, and shift distance $a = 2.0 \text{ mm}$. Based on the famous ultrasonic immersion transmission technique [9], the entire set-up was immersed in water. The generating and receiving immersion transducers (Shantou Institute of Ultrasonic Instruments, diameter 25.4 mm, central frequency 1.0 MHz) were placed close to the sample surface away from which were 4 mm and 2 mm, respectively. A pulser/receiver (Panametrics model 5800) produced a short duration (about 0.4 ms/ pulse which was applied to the generating transducer launching the probing longitudinal waves. The signal acquired by the receiving transducer was digitized with a sampling rate of 100 MHz by a digital oscilloscope (Tektronix TDS 3032 B). To reduce the random errors, 512 measurements were averaged before a Fast Fourier Transform (FFT) was performed to obtain the transmission spectra. In our experiment, the system was first calibrated with no sample. Two transducers should be aligned and the surfaces of each transducer and the sample should be parallel to each other. The reference signal was obtained by recording a pulse with the sample removed from the experimental set-up, i.e., the reference signal propagated through just water, under keeping two transducers immovable as having sample.

4. RESULTS AND DISCUSSION

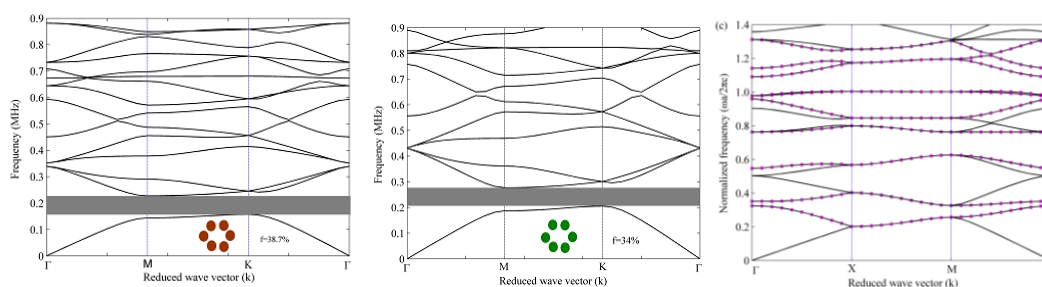


Figure 2. Acoustic band structures of infinite PCs composed of steel rods in water. (a) Hybrid honeycomb lattice, with the shift distance $d=7/9h$, h denotes the height of honeycomb. The lattice constant, radius of steel rods and filling fraction are $a = 2.5 \text{ mm}$, $r=1 \text{ mm}$, respectively. The dashed region represents the complete stop band. (b) honeycomb lattice, with the same lattice constant and filling fraction as (a) and (c)

Firstly, we calculate the band structure of PC of our constructed honeycomb structure (Fig. 2(a)) at the same lattice constant and different filling fraction, i.e. $a = 2.5\text{mm}$, $f = 34\%$ and $f = 38.7\%$ respectively. As shown in Fig. 2(a), an absolute band gap appears from 0.205-0.277 MHz and from 0.157-0.227 MHz between the first and the second bands for honeycomb lattice to the different filling fraction $f = 34\%$ and $f = 38.7\%$ respectively. Corresponding the directional band gap of Γ -K and Γ -M are 0.205-0.296 MHz and 0.187-0.277 MHz for filling fraction $f = 34\%$ and 0.157-0.242 MHz and 0.144-0.227 MHz for filling fraction $f = 38.7\%$ respectively. Comparing with these six figures, we can see that filling fraction increase can lift the band degeneracy in the first BZ. Thus, a low-frequency band gap can open for the honeycomb structure.

Secondly, in Fig. 3 (a) we plot the sound attenuation spectra of these lattices with the FEM computation. The dotted line region show the arisen location of first direction band gap of the Γ -K direction, the frequency range is from 0.21 MHz to 0.29 MHz. this band gap prescribe a limit to the low frequency boundary of the first complete band gap for the two-dimensional honeycomb lattice steel/water PCs, the theoretical calculation result is 0.205-0.296 MHz. The dotted line range showed emerging location of the first direction band gap of the Γ -M direction(0.194-0.285 MHz), it showed in fig. 3(b).this band gap prescribe a limit to the first complete band gap high frequency boundary of 2D honeycomb lattice steel/water PCs. The first direction band gap frequency range is 0.187-0.277 MHz calculated with the PWE.

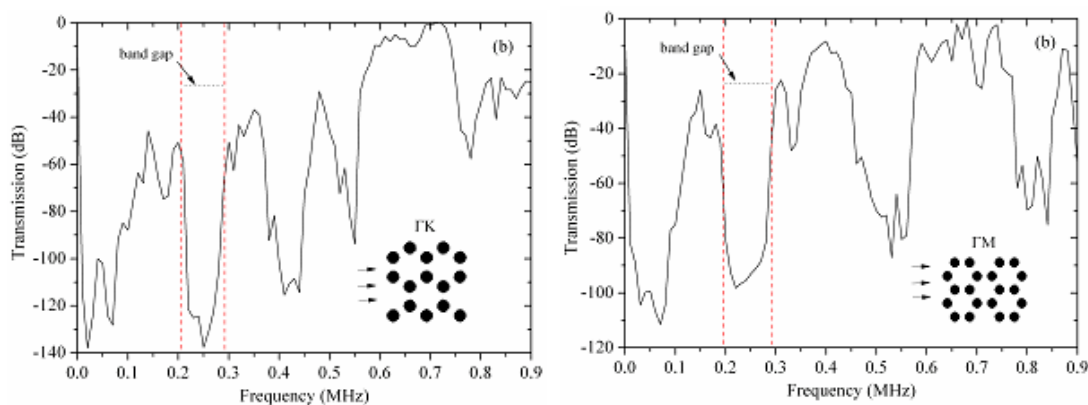


Figure 3. (a) A 2D honeycomb steel-water phononic crystal with the filling fraction 34% in Γ -K and Γ -M direction, (b) its transmission spectrum. The inset shows the direction of incidence of wave launches by the emitting transducer and the cross section of 2D honeycomb steel-water phononic crystal

Fig.3(a) and (b) show that the measured transmission spectra(0.210-0.285 MHz) were found to be in good agreement with the numerical results(0.205-0.277 MHz).fig.1 appear along the Γ -M direction and Γ -K direction, which prescribe a limit to the 2D PCs crystal first complete band gap high frequencies and low frequencies boundary, in Fig.3(b), to Γ -K direction(15 layer) dotted line range show the position of the first direction bandgap, the experimental result was 0.155 -0.250 MHz, the theoretical calculation 0.157-0.242 MHz. The same as to Γ -M direction. the experimental result was

0.15-0.232 MHz, the theoretical calculation 0.144-0.227 MHz. With the filling factor increasing, there is no obvious attenuation for the honeycomb lattice, while appears strong attenuation for the hybrid structure. This also proves that a new band gap opens for the hybrid lattice due to lifting the band degeneracy at X point between the first and second bands.

Next, the first complete band gap's normalization was performed. Through the relative width of band gap ($\Delta\omega/\omega_g$) and normalization radii (r_0/a) to describe the valid band gap[25]. In Fig. 4, the results demonstrated that the the relative width of band gap ($\Delta\omega/\omega_g$) monotonously increased with normalization radii (r_0/a) increasing. The band gap opened when r_0/a equal to 0.21 (amount to the fill factor equal to 10.67%), that was the 2D Honeycomb lattice steel/water PCs easy to obtain low frequencres band gap.

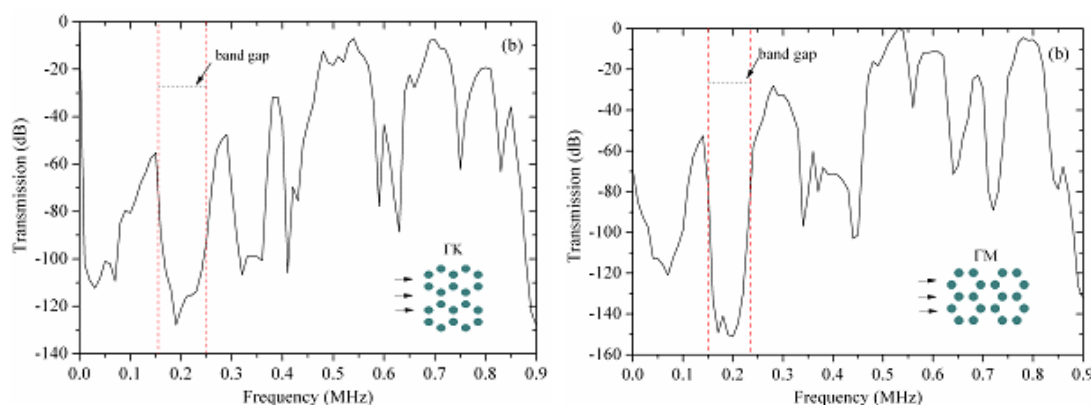


Figure 3. (a) A 2D honeycomb steel-water phononic crystal with the filling fraction 38.7% in Γ -K and Γ -M direction, (b) its transmission spectrum. The inset shows the direction of incidence of wave launches by the emitting transducer and the cross section of 2D honeycomb steel-water phononic crystal

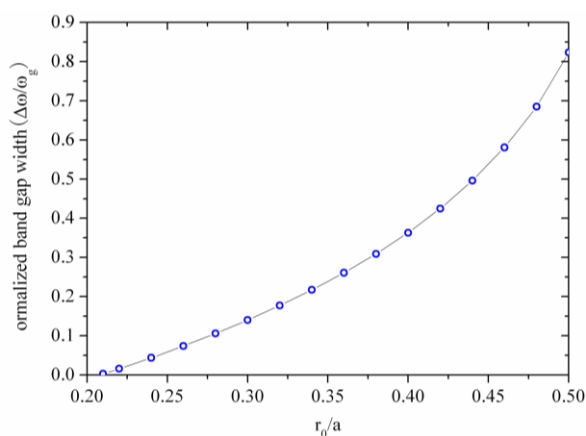


Figure 4. Normalized gap width versus the normalized radius for a 2D steel-water phononic crystal with honeycomb lattice

5. CONCLUSIONS

In summary, the band gap properties of hybrid honeycomb lattice PC consisting of steel rods in water were investigated from the theoretical calculation and experimental results. Due to the symmetry of honeycomb lattice is lower than triangle lattice and the increasing filling factor, a novel low-frequency complete band gap occurs between the first and the second bands for the hybrid structure. The measured transmission spectra in experiment are in agreement with the calculated results. In addition, the effect on measurement band gap of different layers sample is analyzed. According to the current research effort, this study can be used to fabricate the low-frequency filter devices or isolate the low-frequency noise in practical engineering design. The morphologies and crystal of corrosion product films vary in different corrosive media.

ACKNOWLEDGMENT

The authors acknowledge the ministry of science and technology of china for its financial support to the subject, the work was supported by the national natural science funds item of China (Grant no .6872c260)

References

1. M.S. Kushwaha, P. Halevi, G. Martinez, L. Dobrzvnski, B. Diafari-Rouhani, *Phys.Rev. B* 49 (1994) 2313_2322.
2. Z.Y. Liu, X.X. Zhang, Y.W. Mao, Y.Y. Zhu, Z.Y. Yang, C.T. Chan, P. Sheng, *Science* 289 (2000) 1734_1736.
3. M. Maldovan, E.L. Thomas, *Appl. Phys. Lett.* 88 (2006) 251907: 1_3.
4. M.S. Kushwaha, B. Diafari-Rouhani, *J. Sound Vibration* 218 (1998) 697_709.
5. J.O. Vasseur, P.A. Deymier, A. Khelif, Ph. Lamibn, B. Djafari-Rouhani, A. Akjouj, L. Dobrzynski, N. Fettouhi, J. Zemmouri, *Phys. Rev. E* 65 (2002) 056608: 1_6.
6. Z.Z. Yan, Y.S. Wang, C.Z. Zhang, *Acta Mech. Solida Sin.* 21 (2008) 104_109.
7. S. Lin, T.J. Huang, J.H. Sun, T.T. Wu, *Phys. Rev. B* 79 (2009) 094302: 1_6.
8. Z.J. He, F.Y. Cai, Z.Y. Liu, *Solid State Commun.* 148 (2008) 74_77.
9. S.X. Yang, J.H. Page, Z.Y. Liu, M.L. Cowan, C.T. Chan, P. Sheng, *Phys. Rev. Lett.* 88(2002) 104301: 1_4.
10. V. Espinosa, V.J. Sanchez-Morcillo, K. Staliunas, I. Perez-Arjona, J. Redondo, *Phys. Rev. B* 76 (2007) 140302(R): 1_4.
11. X.H. Wang, B.Y. Gu, Z.Y. Li, G.Z. Yang, *Phys. Rev. B* 60 (1999) 11417_11421.
12. N. Susa, *J. Appl. Phys.* 91 (2002) 3501_3510.
13. A.N. Darinskii, E.L. Clezio, G. Feuillard, *Wave Motion* 45 (2008) 970_980.
14. Z.Y. Li, B.Y. Gu, G.Z. Yang, *Phys. Rev. Lett.* 81 (1998) 2574_2577.
15. T. Trifonov, L.F. Marsal, A. Rodriguez, J. Pallares, R. Alcobilla, *Phys. Rev. B* 69(2004) 235112: 1_11.
16. L.J. Martinez, A. Garcia-Martin, P.A. Postigo, *Opt. Express* 12 (2004) 5684_5689.
17. M.D. Weed, H.P. Seigneur, W.V. Schoenfeld, *Proc. SPIE* 7223 (2009) 72230Q:1_9.
18. W.M. Robertson, G. Arjavalngam, R.D. Meade, K.D. Brommer, A.M. Rappe, J.D. Joannopoulos, *Phys. Rev. Lett.* 68 (1992) 2023_2026.
19. J.V. Sanchez-Perez, D. Caballero, R. Martinez-Sala, C. Rubio, J. Sanchez-Dehesa, F. Meseguer, J. Llinares, F. Galvez, *Phys. Rev. Lett.* 80 (1998) 5325_5328.

20. C. Rubio, D. Caballero, J.V. Sanchez-Perez, R. Martinez-Sala, J. Sanchez-Dehesa, F. Meseguer, F. Cervera, *J. Lightwave Technol.* 17 (1999) 2202_2207.
21. F.L. Hsiao, A. Khelif, H. Moubchir, A. Choujaa, C.C. Chen, V. Laude, *J. Appl. Phys.* 101 (2007) 044903: 1_5.
22. S.Zheng, D.Wang, Y.Qi, C.Chen and L.Chen, *Int.J.Electrochem.Sci*, 7(2012)12857
23. Hsiao Fu-Li, A. Khelif, H. Moubchir, et al., *J. Appl. Phys.*, 101(4) (2007)044903.
24. J.Tang, Y.Shao, J.Guo, T.Zhang, G Meng and F.Wang, *Corros.Sci.* 52(2010)2050.
25. M. Sigalas, E.N.Economou, *Solid State Commun.*, , 86(3) (1993)141-143